Plant Ecology & Diversity
i*First*, 2009, 1–14

Taylor & Francis
Taylor & Francis Group

The role of cost–benefit analysis in models of phytoplankton growth and acclimation

Richard J. Geider[a]*, C. Mark Moore[b] and Oliver N. Ross[c]

[a]*Department of Biological Sciences, University of Essex, Colchester, UK;* [b]*National Oceanography Centre, University of Southampton, Southampton, UK;* [c]*Mediterranean Centre for Marine and Environmental Research (UTM CSIC), Barcelona, Spain*

(*Received 30 May 2009; final version received 28 August 2009*)

Background: A key current issue in pelagic ecosystem modelling is obtaining better representations of the growth of phytoplankton so as to increase our understanding of the links between climate change and ocean biogeochemistry.
Aims: Here we explore the use of cost-benefit analysis within the context of assessing the optimal distribution of resources for maximizing phytoplankton growth.
Methods: We focus on capital and running costs by revisiting some of John Raven's cost-benefit analyses of chloroplast structure/function relations. Then, we describe a general framework for application of cost-benefit considerations in models of phytoplankton growth.
Conclusions: Key to applying optimality criteria to phytoplankton growth models is quantifying the costs and benefits of alternative acclimation strategies. Costs include (1) capital costs of the structural and functional components of the cell, (2) running costs of CO_2 fixation, nutrient acquisition, biosynthesis and repair, (3) opportunity costs for exploiting variability in the environment, and (4) taxes imposed by losses associated with transport to unfavourable environments, grazers and parasites. On short timescales of phytoplankton blooms, benefits can be assessed through influences on net growth rate, which can be increased by maximising resource gain (r-strategy) or minimizing losses (K-strategy). On longer timescales from years to millennia, the benefit is survival.

Keywords: acclimation; cost–benefit; photosynthesis; phytoplankton; resource-allocation

Downloaded By: [Geider, Richard J.] At: 09:45 19 November 2009

Introduction

One of the strands of John Raven's research has been quantitative assessment of the costs and benefits of different biochemical and physiological processes within microalgae and cyanobacteria. These include assessments of the costs and benefits of photon absorption (Raven 1984), transport processes (Raven and Handley 1987), and motility (Raven and Richardson 1984), as well as assessment of the efficiency with which trace metals such as Fe, Mo and Mn are used (Raven 1988, 1990), the costs of photoinhibition (Raven and Samuelsson 1986; Raven 1989) and constraints imposed on growth by size (Raven 1999).

In this contribution, we first discuss the framework for applying cost–benefit analysis in modelling the photosynthetic physiology and growth of microalgae within an oceanographic context. We then present new calculations comparing three hypothetical strategies for optimising light harvesting in constant light, before revisiting aspects of the costs and benefits of photon absorption that were originally examined in two of John Raven's papers that have been a continuing inspiration to the senior author. These are his 1980a paper on 'Chloroplasts of eukaryotic micro-organisms' and his 1984 paper on 'A cost–benefit analysis of photon absorption by photosynthetic unicells'. These papers focused on two types of costs, the capital investments in structural and functional components and the running costs of light harvesting and CO_2 fixation. Finally, we describe a framework for introducing two additional costs, namely opportunity costs and taxes, into cost–benefit models of phytoplankton growth. We conclude by emphasising the potential for applying optimality models to phytoplankton growth and describing some of the challenges that need to be overcome to ground theoretical models in an improved understanding of underlying mechanisms.

Oceanographic context

One goal of oceanographic research is to understand how the ocean carbon cycle has responded to climate change in the past (e.g. glacial to interglacial) and how it will respond to ocean acidification (Raven et al. 2005) and global warming in the future. This goal has led to the development and application of many ocean biogeochemical models (Doney et al. 2003). Central to these models are descriptions of the effects of temperature, light and nutrient limitation on the growth rate and primary productivity of phytoplankton. Also of fundamental importance are descriptions of variability in the phytoplankton carbon/chlorophyll *a* ratio since satellite-based estimates of chlorophyll *a* are frequently used both for estimating contemporary oceanic primary production and phytoplankton growth rates (Westberry et al. 2008), as well as evaluating the performance of global ocean biogeochemical models (e.g. Aumont et al. 2003; Moore et al. 2004). Finally, phytoplankton elemental composition needs to be included in

*Corresponding author. Email: geider@essex.ac.uk

ISSN 1755-0874 print/ISSN 1755-1668 online
© 2009 Botanical Society of Scotland and Taylor & Francis
DOI: 10.1080/17550870903300949
http://www.informaworld.com

biogeochemical models since the carbon cycle in the ocean is intricately linked to the cycles of potentially limiting nutrients (N, P, Fe, and in the case of diatoms, Si) (Falkowski et al. 1998; Moore et al. 2004).

Most ocean biogeochemical models use empirical descriptions of the effects of resource limitation on phytoplankton growth (Friend et al. 2009) such as the Monod equation and cell quota models. These empirical models can be rationalised in terms of underlying physiological mechanisms, and choice of appropriate parameter values informed by cell size through allometric scaling arguments (Aksens and Egge 1991; Klausmeier et al. 2004; Litchman et al. 2007). It has been suggested that these simple representations may need to be replaced by models that include more sophisticated treatments of the interactions amongst limiting factors and physiological acclimation (Hood et al. 2007). Although mechanistic models of phytoplankton growth have been developed (e.g. Flynn 2001), such models are often too detailed for inclusion in ocean biogeochemical models (Flynn 2003). Alternatively, physiology can be modelled as a trade-off in resource allocation amongst different metabolic functions to maximise growth rate (Shuter 1979; Klausmeir et al. 2004; Pahlow 2005; Armstrong 2006; Pahlow and Oschlies 2009). Armstrong (2006) suggested that optimality-based phytoplankton growth models that account for trade-offs in resource allocation can be simple enough to be employed in ocean biogeochemical models, yet sophisticated enough to be used to assess competition amongst different functional groups.

Optimality models: evolutionary fitness versus physiological fitness

Central to optimality models is the assumption that evolution by natural selection favours organisms that possess optimal traits that maximise evolutionary fitness. Evolutionary fitness is commonly defined as the probability that a particular genotype will have descendants in future generations. Applying optimality criteria in models of phytoplankton growth thus requires that we develop quantitative descriptions of the costs and benefits of various traits so that the optimal combination can be predicted. Since the optimal outcome is defined as the one that maximises fitness, a complete definition of the fitness function that is to be maximised is required, potentially leading to considerable difficulty. For example, in complex natural environments, it may be necessary to reconcile conflicting constraints, and thus to satisfy more than one fitness function. On annual and longer timescales, the net population growth rate will be approximately zero, and fitness will be related to persistence. However, persistence may be achieved by satisfying an evolutionary fitness function (e.g. persistence through annual cycles) rather than maximising a physiological function (e.g. net growth rate). Moreover, the selection pressures that have resulted in the persistence of genotypes will not necessarily have acted to optimise physiological rates or biogeochemical fluxes under local conditions. Lack of comparability can be an issue here.

When it comes to understanding the role of phytoplankton in ocean biogeochemistry, it is not sufficient to understand the traits that contribute to evolutionary persistence. It is also necessary to understand the traits that lead to local dominance in space and/or in time (e.g. blooms). In this case, fitness may be equated to net population growth rate. These considerations lead to a range of important questions. How does one compare the costs and benefits of traits that contribute to net population growth with those that contribute to persistence? Is it necessary to define one fitness function for net growth of vegetative stages, another for persistence of cysts or resting stages, and a third function to trigger transitions between growing (e.g. vegetative) and persisting (e.g. cyst or resting) stages?

Clearly the problem under investigation, the timescales of heterogeneity in the natural environment (e.g. patchiness of resources, predators) and the timescales to which the model is to be applied (e.g. seasonal cycle, interannual and interdecadal oscillations, climate change) need to be taken into account when defining a fitness function. Although the timing and location of phytoplankton blooms are often predictable from changes in ocean physics (e.g. mixing and stratification), a high degree of non-linear interactions, approximating 'random chance', may influence the phytoplankton genotypes that come to local dominance (Harris 1986). These processes may include the presence of seed populations of different phytoplankton taxa, the genetic variability within these taxa, and/or the presence/absence of parasites and predators that preferentially infect or feed upon different taxa. Maximising net growth rate may thus be an important characteristic for the formation of blooms which disproportionately contribute to biogeochemical fluxes; however it is unlikely to be the only one.

For the remainder of the current contribution we principally focus on cost–benefit analyses in the context of optimising net growth rates over physiologically relevant timescales. Specifically we consider trade-offs in the acclimation of chloroplast function. By implication our focus is thus on processes which operate on timescales of hours to weeks. However, we later return to discussion of the ecological/evolutionary context, which we suggest may be at least as important as physiological optimality, particularly over longer timescales.

Optimising light harvesting in constant light

The simplest situation for defining a fitness function and specifying the criteria for optimisation is for growth of an axenic phytoplankton population in the constant environment of a chemostat culture. Under these conditions, balanced growth is attained and the specific rates of increase of all indices of biomass are identical:

$$\mu = \frac{1}{A}\frac{dA}{dt} = \frac{1}{B}\frac{dB}{dt} = \cdots = \frac{1}{X}\frac{dX}{dt} \qquad (1)$$

where μ is the specific growth rate (see Table 1 for list of symbols and units), and A, B, . . . X are indices of cell

Downloaded By: [Geider, Richard J.] At: 09:45 19 November 2009

Table 1. Definitions of symbols, together with the number of the equation where the symbol appears first.

Symbol	Definition	Equation
a^{chl}	Chlorophyll *a*-specific light-absorption coefficient (with units of m^2 (g Chl *a*) $^{-1}$)	11
α^{chl}	Chlorophyll *a*-specific initial slope of the P vs. E curve (with units of [m^2 (g Chl *a*)$^{-1}$] [g C (μmol photons)$^{-1}$])	2
Chl:C or $\frac{Chl}{C}$	Chlorophyll *a* to carbon ratio	2
χ_{Chl}	Carbon to chlorophyll *a* ratio of the light-harvesting apparatus	3
E	Irradiance (with units of μmol photons m^{-2} s^{-1})	2
E_k	Light-saturation parameter	2
ϕ	Quantum efficiency of photosynthesis (with units of mol C (mol photons)$^{-1}$)	11
Λ_{LH}	Proportion of cellular biomass associated with light harvesting	3
Λ_{Con}	Proportion of cellular biomass in constitutive components	4
μ	Specific growth rate (with units of inverse time)	1
μ_m	Maximum value of the specific growth rate	4
P^C	Carbon-specific photosynthesis rate (with units of inverse time)	2
P_m^C	Maximum value of the carbon-specific photosynthesis rate	2
R^C	Carbon-specific respiration rate (with units of inverse time)	2
syn_{max}	Biosynthetic capacity (with units of inverse time)	4

Downloaded By: [Geider, Richard J.] At: 09:45 19 November 2009

biomass (e.g. cell abundance, organic carbon, chlorophyll *a*). In fact, several applications of optimality models to understanding phytoplankton growth have been applied to this situation (Shuter 1979; Pahlow 2005; Armstrong 2006). In a constant environment offered by a chemostat culture, competition will select the genotype with the highest cell division rate. Here the fitness function is the specific growth rate.

When the fitness function is the specific growth rate, μ, and the cell is optimising resource acquisition, the benefit can be defined as the increment in μ that arises from an investment in a component of the cell that limits growth. When light is a limiting resource, growth rate can be enhanced by investment in light-harvesting pigments such as chlorophyll *a*, which increases the ratio of chlorophyll *a* to carbon (Chl:C). The benefit of an increase in Chl:C is increase in the biomass-specific net CO_2 fixation rate which is given by a photosynthesis light response curve such as:

$$P^C = P_m^C \cdot \left(1 - \exp\left(\frac{-\alpha^{Chl} \cdot \frac{Chl}{C} \cdot E}{P_m^C}\right)\right) - R^C = P_m^C \cdot \left(1 - \exp\left(\frac{-E}{E_K}\right)\right) - R^C \quad (2)$$

where P^C is the C-specific CO_2 fixation rate, P_m^C is the light-saturated rate, E is the photon flux density, α^{Chl} is the chlorophyll *a*-specific initial slope of the photosynthesis versus light curve, Chl:C is the ratio of cellular chlorophyll *a* to cellular C, E_K is the light saturation parameter, and R^C is the respiration rate (see Table 1).

In equation (2), Chl represents the light-harvesting component of the phytoplankton cell. We can designate the proportion of cellular biomass contained in this component as Λ_{LH}. We assume that Λ_{LH} consists of chlorophyll *a* and accessory pigments contained within pigment protein complexes, together with the supporting thylakoid membrane lipids and photosynthetic electron transfer (PET) proteins, and that the value of Λ_{LH} is given by:

$$\Lambda_{LH} = \chi_{Chl} \cdot \frac{Chl}{C} \quad (3)$$

where χ_{chl} is the ratio of carbon to chlorophyll *a* in the light-harvesting apparatus.

In addition to the light-harvesting component, we assume that the cell contains a constant proportion of constitutive components, Λ_{Con}. For a cell of constant biovolume and biomass, the plasma membrane, cell wall and genetic material would be expected to account for constant proportions of biomass. This allows us to define the proportion of the non-constitutive, non-light-harvesting component of the cell as $(1 - \Lambda_{Con} - \Lambda_{LH})$. To obtain the optimal distribution of resources between the light harvesting and the remaining non-constitutive components of the cell, we start by assuming that increasing Λ_{LH} imposes a cost because it sequesters a proportion of cellular biomass that would otherwise be available for other purposes. In other words, the cost of increasing Chl:C is the diversion of resources away from other compounds. We also assume that this cost is proportional to $(1 - \Lambda_{Con} - \Lambda_{LH})$, i.e. we assume that the cost of diversion of resources from any component pool is proportional to the reduction in size of that pool. We consider three alternative scenarios for increasing Chl:C, involving the diversion of resources from the cellular pools which provide the biomass to support either the maximum capacity for biosynthesis (scenario 1), the light-saturated CO_2 fixation rate (scenario 2), or the capacity for protection from light-induced damage (scenario 3). These alternative scenarios represent several

ways that might be employed to allocate resources within a phytoplankton cell to solve the 'local' problem of maximising μ under constant environmental conditions imposed in a chemostat. The 'global' response achieved on evolutionary timescales in the natural environment, which ultimately shapes the genome, may not conform to this logic. The three scenarios that are considered are hypothetical and to some extent arbitrary, however they have been chosen for their simplicity and because they encompass several possible alternative constraints on photosynthesis and growth.

Scenario 1: trade-off between light harvesting and the capacity for biosynthesis

In this scenario, we assume that the maximum growth rate is proportional to cellular biomass which is not constitutive or associated with light harvesting, $(1 - \Lambda_{Con} - \Lambda_{LH})$, as follows:

$$\mu_m = syn_{max} \cdot (1 - \Lambda_{Con} - \Lambda_{LH}) \quad (4)$$

where syn_{max} is the maximum biosynthetic capacity. For example, if (1) growth rate was limited by the rate of protein synthesis, (2) protein synthesis was limited by the proportion of cellular biomass contained within ribosomes, and (3) ribosomal mass was proportional to $(1 - \Lambda_{Con} - \Lambda_{LH})$, then we could calculate syn_{max} from the ribosomal efficiency. As far as we are aware, the data to make such a calculation are not available for any phytoplankter, and as a consequence we can estimate a value for syn_{max} from $syn_{max} = \mu_m/(1 - \Lambda_{Con} - \Lambda_{LH})$. Under this scenario, an increase in Chl:C thus comes at the expense of a decline in the achievable maximum growth rate μ_m, which has an upper limit of $\mu_{max} = syn_{max}\ (1 - \Lambda_{Con})$ when $\Lambda_{LH} = 0$.

If the balanced growth rate under constant light is the minimum of the net photosynthetic CO_2 fixation rate and the biosynthesis rate, then the specific growth rate is given by the minimum function:

$$\mu = \text{Minimum}\left[\begin{array}{c} P_m^C \cdot \left(1 - \exp\left(\frac{-E}{E_K}\right)\right) - R^C \\ \mu_m \end{array}\right] \quad (5)$$

Thus, the balanced growth rate is constrained either by light-limitation of the rate of CO_2 assimilation which increases with Chl:C, or by a limitation on the maximum rate of biosynthesis, which declines with increases in Chl:C (Figure 1). The optimal Chl:C is found when:

$$P_m^C \cdot \left(1 - \exp\left(\frac{-E}{E_K}\right)\right) - R^C = syn_m \cdot (1 - \Lambda_{Con} - \Lambda_{LH}) \quad (6)$$

Scenario 2: trade-off between light harvesting and the capacity for light-saturated photosynthesis

In this scenario we assume that the light-saturated photosynthesis rate is proportional to $(1 - \Lambda_{Con} - \Lambda_{LH})$. Instead of assuming a constant value of P_m^C as in equation (2), in this scenario we define P_m^C as follows:

$$P_m^C = P_{max}^C \cdot (1 - \Lambda_{Con} - \Lambda_{LH}). \quad (7)$$

In this case, the catalysts for biosynthesis are assumed to be expressed constitutively and included in Λ_{Con}. We also assume that the maximum capacity for biosynthesis never limits the achieved growth rate. In this case, the maximum biomass specific growth rate, μ, will be found at the optimal Chl:C where the net photosynthesis rate, P^C (equation (2)), is a maximum (Figure 1).

Scenario 3: trade-off between light harvesting and the capacity for photoprotection

Finally, we consider a scenario where the capacity for protection from light-induced damage is proportional to $(1 - \Lambda_{Con} - \Lambda_{LH})$. As in scenario 2, we assume that the biosynthetic capacity never limits the growth rate. We also assume that the catalysts that determine the light-saturated photosynthesis rate are expressed constitutively, and as in scenario 1 that P_m^C is constant. In scenario 3, we recognise that light is not only a resource but also a potential source of photo-oxidative damage. We assume that the damage rate is proportional to the rate of light absorption, and thus to $\Lambda_{LH}\,E$, but inversely proportional to the capacity for photoprotection, which is given by $(1 - \Lambda_{Con} - \Lambda_{LH})$:

$$\mu = P_m^C \cdot \left(1 - \exp\left(\frac{-E}{E_K}\right)\right) - R^C - \frac{d \cdot \frac{Chl}{C} \cdot E}{(1 - \Lambda_{CON} - \Lambda_{LH})} \quad (8)$$

where d is the damage coefficient. In this formulation of light stress, we express the cost of the light-induced damage as a diversion of photosynthate from growth-related processes. In this case, the optimal Chl:C is obtained where μ (equation (8)) is a maximum (Figure 1).

All three of these hypothetical scenarios for modelling the optimal Chl:C under balanced growth yield results that are qualitatively similar to observations (Figure 2). This exercise thus illustrates the potential for applying optimality considerations to photoacclimation, but also demonstrates the need for more mechanistic information on the underlying processes. The reality may be that all three scenarios apply, but to variable extents. However we cannot preclude the possibility that other scenarios apply. The analysis also illustrates that similar optimal Chl:C ratios can be

Downloaded By: [Geider, Richard J.] At: 09:45 19 November 2009

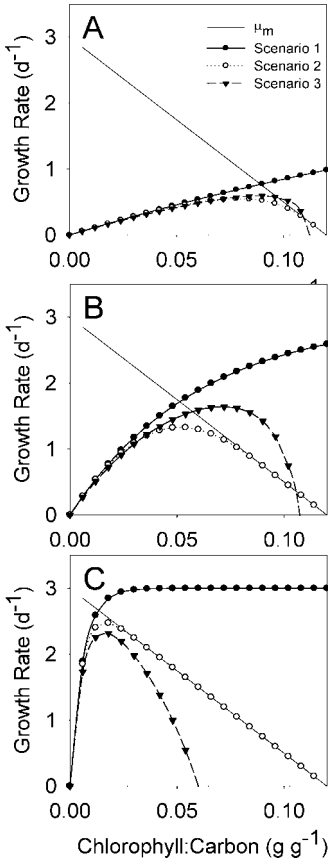

Figure 1. Determination of the optimal Chl:C for scenarios in which the cost of increasing Chl:C is assumed to be due to a reduction in the capacity for biosynthesis (scenario 1), a reduction in the maximum capacity for light-saturated photosynthesis (scenario 2) or a reduction in the capacity to prevent or repair light-induced damage (scenario 3). For scenario 1, the optimal value is given by the intercept of the straight diagonal line from upper left to lower right with the saturating line with closed circles rising from lower left to upper right. For the other scenarios, the optimal Chl:C is the value that yields the maximum growth rate. Balanced growth rate was calculated as a function of Chl:C for photon flux densities of (A) 20 µmol photons m^{-2} s^{-1}, (B) 100 µmol photons m^{-2} s^{-1} and (C) 1,000 µmol photons m^{-2} s^{-1}. The parameter values used in these simulations were as follows: μ_{max} = 2.5 d^{-1} (scenario 1), $P_m^C = 3\ d^{-1}$ (scenarios 1 and 3), $P_m^C = 5 d^{-1}$ (scenario 2 only), syn_{max} = 5 d^{-1}, α^{Chl} = 7.5 10^{-6} m^2 (g Chl)$^{-1}$ (g C)(µmol photons m^{-2} s^{-1})$^{-1}$, Λ_{con} = 0.4, χ_{Chl} = 5 g C (g Chl)$^{-1}$, R^C = 0, and d = 0.015 (g C) (g Chl d)$^{-1}$ (µmol photons m^{-2} s^{-1})$^{-1}$ (scenario 3).

obtained from different sets of assumptions regarding the cost functions. Thus, comparison of the model output with observations for balanced growth may not be sufficient to obtain information on the mechanisms that account for acclimation of Chl:C to light. However, other biological knowledge can be used to support or refute specific mechanisms. For example, limited variability in the ribulose bisphosphate carboxylase/oxygenase (RuBisCO) and RNA contents of phytoplankton in response to growth at different photon flux densities (see Harris et al. 2009) appears to be inconsistent with the assumptions of both scenarios 1 and 2.

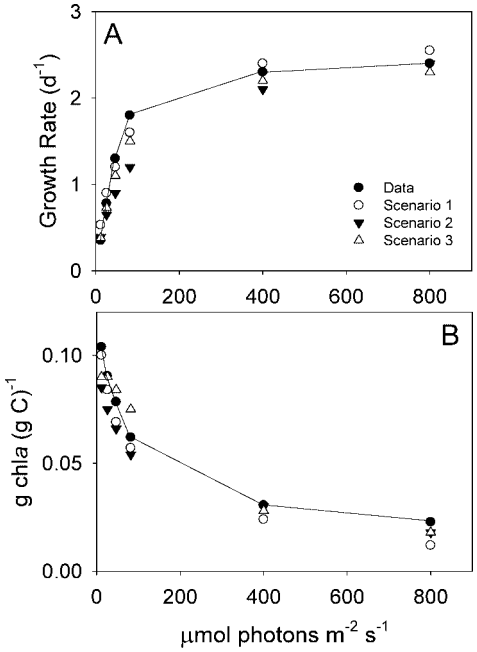

Figure 2. Comparison of data for *Chlorella pyrenoidosa* with calculations of the optimal Chl:C and corresponding growth rates obtained from the three optimality scenarios illustrated in Figure 1 (using the parameter values given in Figure 1). Observations of growth rate were taken from Myers and Graham (1971), whereas chlorophyll to carbon ratio was estimated from the sum of chlorophylls *a*+*b* to dry weight, assuming that carbon accounted for 50% of the dry weight. Photon flux densities were estimated using information given in Myers and Graham (1971).

Cost–benefit analysis of chloroplast function

As described above, applying optimality criteria to understanding phytoplankton growth requires quantitative, preferably mechanistic, descriptions of the costs and benefits of various traits so that the optimal combination can be predicted. In assessing the costs and benefits of photoacclimation of pigment content, a good place to start is Raven's (1980a) paper on 'Chloroplasts of eukaryotic micro-organisms'. In this paper, Raven analysed the structure–function relationships of chloroplasts within the context of three design constraints. These constraints were:

- catalytic efficiency defined as 'the work output per unit of catalytic and structural material used',
- energetic efficiency defined as 'the intrinsic efficiency of the process, i.e. the ratio of useful work output to energy input', and
- 'safety' because "otherwise advantageous mechanisms with local or global optimal balance of the first two design features might, in the long term, be too risky." (p. 183)

In addition to specifying design constraints, it is essential to define the fitness functions (in other words the benefits) that are being optimised, and the structures within the cell

Downloaded By: [Geider, Richard J.] At: 09:45 19 November 2009

that perform these functions. The major functions of chloroplasts are

- to use light energy to produce reductant (e.g. nicotinamide adenine dinucleotide phosphate [NADPH]) and high-energy phosphate bonds (e.g. adenosine triphosphate [ATP]),
- to use NADPH and ATP generated by the light reactions to fix CO_2 into triose phosphates, and
- to export energy in the form of triose-P, reducing equivalents and ATP to the rest of the cell for use in biosynthesis and maintenance.

The structures that allow these functions to take place are the thylakoid membranes, the chloroplast envelope, and the stroma.

Raven (1980a) identified two types of costs, capital costs and running costs. Where the benefit to be maximised is the rate of CO_2 fixation, the capital costs are affected by the catalytic efficiencies of the components of the photosynthetic apparatus and the requirements for structural materials such as membrane lipids, whereas the running costs are affected by the energetic efficiency of photosynthesis.

Running costs of CO_2 fixation and the maximum photon efficiency of CO_2 fixation

Complicating a comparison of running costs with benefits of CO_2 fixation are the different currencies for energy employed by chloroplasts. Energy enters the cells in the currency of photons, is converted to the currencies of reducing equivalents in NADPH and high energy phosphate bonds of ATP by the light reactions of photosynthesis, and subsequently used to fix CO_2 into organic matter, the rate of which is expressed in the currency of carbon.

Photosynthesis uses light energy to produce both NADPH and ATP. These two products of the light reactions are produced in variable amounts depending on the metabolic requirements of the cells (Behrenfeld et al. 2004, 2008; Baker et al. 2007). They are consumed during photosynthetic CO_2 fixation, photorespiratory O_2 consumption, nutrient assimilation and biosynthesis. Here we limit ourselves to considering the sink associated with CO_2 fixation.

The pathway of photosynthetic reductant formation is located on the thylakoid membranes and is referred to as linear photosynthetic electron transfer (LPET). All of the reducing equivalents required by a photoautotrophic cell are ultimately derived from LPET, and as such can be traced to the splitting of water to produce O_2, H^+ and e^- in PSII. The Z-scheme of photosynthesis describes PET from water to NADPH (Figure 3A). ATP is produced in parallel to the production of NADPH, using the energy associated with transfer of protons across the thylakoid membrane, which occurs in conjunction with LPET (Baker et al. 2007). The generation of NADPH and ATP by the Z-scheme can be summarised as:

$$2\,H_2O + 2\,NADP^+ + 2.6\,ADP + 2.6\,P_i + 8\,photons \rightarrow O_2 + 2\,NADPH + 2.6\,ATP + 4H^+. \quad (9)$$

Carbon fixation via the Calvin cycle consumes 2 NADPH and 3 ATP for each CO_2 fixed (Baker et al. 2007).

$$CO_2 + 2\,NADPH + 3\,ATP + 4\,H^+ \rightarrow CH_2O + H_2O + 2\,NADP^+ + 3\,ADP + 3\,P_i. \quad (10)$$

Note that LPET from water to NADPH (as depicted in equation (9)) does not produce enough ATP to power CO_2 fixation (equation (10)).

To maximise the rate of CO_2 fixation by the Calvin cycle, the oxygenase activity of RuBisCO must be suppressed. This is achieved in many microalgae though operation of a CO_2-concentrating mechanism (CCM;

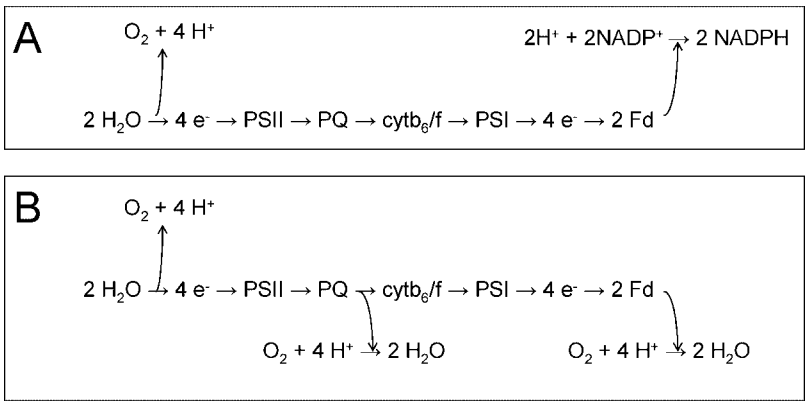

Figure 3. Electron transfer pathways from water to the terminal electron acceptors. (A) Z-scheme for photosynthesis, linking water splitting by photosystem II to production of nicotinamide adenine dinucleotide phosphate (NADPH). (B) Linear photosynthetic electron transfer (LPET) from H_2O to H_2O (water–water cycles) via either the plastoquinone terminal oxidase (PTOX) or the Mehler reaction.

Downloaded By: [Geider, Richard J.] At: 09:45 19 November 2009

Raven 1997; Raven and Johnston 1991; Raven et al. 2008). However, the CCM requires ATP, and this requirement exacerbates the imbalance between the provision of ATP and NADPH by LPET from H_2O to NADPH with the demand for CO_2 fixation. So, for example, if 1 ATP per CO_2 fixed is required for operation of the CCM then 4 ATP and 2 NADPH are required for the fixation of each molecule of CO_2 into triose-P.

Photoautotrophs supplement LPET from H_2O to NADPH with additional light-driven generation of ATP (Baker et al. 2007). Two of the processes that can generate this additional ATP involve the reduction of O_2 by the PET chain: these processes involve either 'mid-stream oxidases' (MOX, Behrenfeld et al. 2008), such as the plastoquinone terminal oxidase (PTOX), or the transfer of e^- from reduced ferredoxin to O_2 in the Mehler reaction (Figure 3B). A third process that can generate the additional ATP is cyclic photosynthetic electron transfer (CPET). The efficiencies with which these processes generate ATP are summarised in Table 2. CPET appears to be the most efficient mechanism for generating this additional ATP, followed by the water–water cycle linked to the Mehler reaction. When the ATP requirement is less than the maximum potential rate at which ATP can be produced, the H^+ gradient across the thylakoid membrane can be dissipated without generating ATP (e.g. Kramer et al. 2004), reducing the photon efficiencies from the maximum values given in Table 2.

It is worth noting that, as with many other physiological interactions, it is likely that costs associated with additional ATP generation will vary depending on the availability of resources other than light. For example, due to the potentially higher requirement for iron-rich photosystem I (PSI) to drive either CPET or Mehler activity, ATP generation via MOX might be favoured in low iron environments (Bailey et al. 2008; Behrenfeld et al. 2008; Mackey et al. 2008).

The theoretical minimum photon requirement for CO_2 fixation is 8 photons to generate 2 NADPH + 2.57 ATP plus 1.7 photons for CPET to provide additional 1.43 ATP giving 9.7 mol photons (mol CO_2 fixed)$^{-1}$. Thus, the maximum photon efficiency, which is the inverse of the minimum photon requirement, is 0.10 mol CO_2 (mol photons)$^{-1}$. However, if the water–water cycle involving the Mehler reaction is used instead of CPET to generate the additional ATP, then the maximum photon efficiency would drop to 0.08 mol CO_2 (mol photons)$^{-1}$. These calculations assume that the use of excitation energy from absorbed photons for photochemistry in PSI and photosystem II (PSII) occurs with 100% efficiency, whereas losses of excitation energy to heat and fluorescence will lead to lower efficiencies. However, the exquisite observations of the photon efficiency for growth of *Chlorella* (Myers 1980), suggest that achieved maximum efficiencies can be close to the theoretical values. Nonetheless, the achieved photon efficiency is likely to be less than this at low light due to the non-linear nature of the photosynthesis-light response curve (equation (2)). At a saturating irradiance, the efficiency will be significantly less.

Capital requirements for light absorption

At very low light, the rate-limiting step in photosynthesis will be the rate of light absorption, and the appropriate catalytic efficiency to consider is the initial slope of the photosynthesis–light response curve. When normalised to chlorophyll *a*, the initial slope provides a convenient index of the maximum catalytic efficiency for light utilisation. All the chlorophyll *a* molecules within a cell are contained in pigment protein complexes, and thus the capital cost is much greater than simply the cellular chlorophyll *a* content alone. We can estimate the carbon content of the light-harvesting apparatus from information on cellular chlorophyll *a* together with information on the protein complexes to which the chlorophyll is bound and the lipid bilayer of the thylakoid membrane within which these pigment–protein complexes are embedded. John Raven undertook such an analysis in his 1984 paper on 'A cost benefit analysis of photon absorption by photosynthetic unicells'. Here we update this analysis for a chlorophyte.

Most of the chlorophyll *a* and accessory pigments are contained in three types of pigment–protein complexes. These are the reaction centre complexes of PSI and PSII (RCI and RCII, respectively) and the antennae complexes associated with these reaction centres. In chlorophytes, these complexes consist of proteins, chlorophyll *a* and accessory pigments including chlorophyll *b*, lutein and

Table 2. Maximum photon efficiencies of adenosine triphosphate (ATP) synthesis associated with linear photosynthetic electron transfer (LPET) to nicotinamide adenine dinucleotide phosphate (NADPH) and O_2 (after Baker et al. 2007).

Electron transfer processes	mol NADPH/mol photons	mol ATP/mol photons	net mol O_2/mol photons
LPET to NADPH	0.25	0.32	0.125
LPET to O_2 (Mehler)	0	0.32	0
LPET to O_2 (via PTOX)	0	0.21	0
CPET	0	0.43–0.86	0

Abbreviations: CPET: cyclic photosynthetic electron transfer; PTOX: plastoquinone terminal oxidase.
Notes: Calculation of ATP production for LPET to NADPH or O_2 via the Mehler reaction is based on development of a proton gradient of 12 H^+/8 photons and generation of 3 ATP/14 H^+ by the thylakoid ATPsynthase. Calculation of ATP production for LPET to O_2 via PTOX is based on development of a proton gradient of 8 H^+/8 photons and generation of 3 ATP/14 H^+ by the thylakoid ATPsynthase. Calculation of ATP production via CPET is based on development of a proton gradient of 2 to 4 H^+/photon cycled around photosystem I and generation of 3 ATP/14 H^+ by the thylakoid ATPsynthase.

Downloaded By: [Geider, Richard J.] At: 09:45 19 November 2009

zeaxanthin. In addition, the thylakoid membranes contain the cytochrome $b_{6/f}$ complex, the ATP synthase, mobile electron carriers, other proteins and supporting lipids. As a specific example, we consider the proportion of cellular C associated with the thylakoid membrane catalysts for the chlorophyte *Dunaliella tertiolecta* based on data provided by Sukenik et al. (1987). We used the information on cellular chlorophyll *a*, chlorophyll *b*, RCII, RCI and cytochrome *f* to calculate the proportions of cellular C associated with the light-harvesting apparatus. The results of our calculations are shown in Figure 4, and the assumptions used in the calculations are described in the figure legend. These show that over 30% of cellular C may be associated with the thylakoid membranes at low light, with most of the carbon devoted to light harvesting functions of the photosynthetic pigments and the antennae proteins, with smaller amounts in the reaction centre complex proteins, other electron transfer proteins and the thylakoid membrane lipids. This is likely to be an underestimate of the proportions of cellular C associated with the thylakoid membranes because we have not accounted for the ATP synthase or the other thylakoid proteins. We obtained an estimate for the carbon to chlorophyll *a* ratio of the light-harvesting apparatus (e.g. χ_{chl} in equation (3)) of about 5 g C (g Chl *a*)$^{-1}$ for the light-harvesting and PET components of the thylakoid membrane of *Dunaliella tertiolecta* from information given in the legend of Figure 4. Similar calculations have recently been made for a diatom, but using a less complete data set (Ross and Geider 2009).

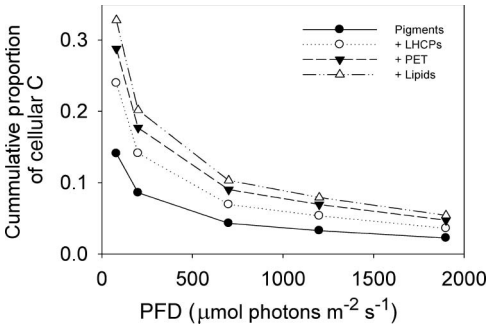

Figure 4. Partial accounting of the distribution of C amongst thylakoid membrane components in *Dunaliella tertiolecta*. Shown are the cumulative proportions of cellular C in photosynthetic pigments (closed circles), plus light-harvesting complex proteins (LHCPs: open circles), plus photosynthetic electron transfer chain (PET; closed inverted triangles), plus thylakoid lipids (open triangles). The amount of carbon associated with light-harvesting pigments was calculated from the cellular contents of chlorophylls *a* and *b* reported by Sukenik et al. (1987) and the assumption that lutein was present in a 2:1 molar ratio to chlorophyll *a*. The cellular contents of reaction centre II (RCII), reaction centre I (RCI), and cyt *f* were reported by Sukenik et al. (1987). The cellular carbon associated with the thylakoid electron transfer complexes was calculated using molecular weights of 368 kDa for the PSII complex, 104 kDa for the cyt b_6/f complex and 289 kDa for the photosystem I (PSI) complex (Blackenship 2002) assuming that proteins are 56% C by weight. The amount of LHCP content was estimated from the cellular chlorophyll *a*, after correcting for the chlorophyll *a* associated with the core complexes of photosystem II (36 per RCII) and PSI (96 per RCI) by assuming a typical molecular weight of 24 kDA for the LHCPs, with each LHCP binding 7 chlorophyll *a* molecules (Blackenship 2002). The thylakoid lipid content was estimated assuming a weight ratio of 0.19 g lipid per gram protein in the thylakoid membranes (Raven 1984), with lipid being 76% C by weight. A cellular carbon content of 30 pg C cell^{-1} reported by Falkowski and Owens (1980) for *D. tertiolecta* growing at photon flux densities of 60–400 μmol photons m^{-2} s^{-1} was used to calculate the proportions of cellular C associated with these components of the thylakoid membranes. If, however, the measured cellular volume of 75 μm^3 reported by Berner et al. (1989) is converted to C using a ratio of 0.26 pg C μm^{-3}, a value of 20 pg C cell^{-1} is obtained. If this C content is used, then the proportions of cell C accounted for by these thylakoid components would increase by 50%.

Catalytic efficiency of CO_2 fixation under low light

In the absence of light-dependent reductions in the photon efficiency of photosynthesis, the light-limited carbon-specific CO_2 fixation rate would be given by:

$$P^C = \alpha^{Chl} \cdot \frac{Chl}{C} \cdot E = 12 \cdot \phi_m \cdot a^{Chl} \cdot \frac{Chl}{C} \cdot E \qquad (11)$$

where P^C is the carbon-specific photosynthesis rate (units of s^{-1}), α^{chl} is the initial slope of the photosynthesis-light response curve (units of [m^2 (g Chl *a*)$^{-1}$][g C (μmol photons)$^{-1}$]), ϕ_m is the maximum photon efficiency of CO_2 fixation (units of [mol CO_2][mol photons]$^{-1}$), a^{Chl} is the chlorophyll *a* specific light absorption coefficient (units of m^2 [g Chl *a*]$^{-1}$) and Chl:C and E have units of [g C][g Chl *a*]$^{-1}$ and [μmol photons m^{-2} s^{-1}] respectively.

As described above, the theoretical maximum value of ϕ_m is 0.10 mol CO_2 (mol photons)$^{-1}$. The value of a^{Chl} varies with the pigment complement of the cell and cell size. For the chlorophyte *Dunaliella tertiolecta*, a^{Chl} has an average value of about 10 m^2 (g Chl *a*)$^{-1}$ across the photosynthetically active waveband (400–700 nm) (Berner et al. 1989). The maximum value of Chl:C observed in *D. tertiolecta* is approximately 0.08 g Chl *a* (g C)$^{-1}$ (Falkowski and Owens, 1980). Thus, at an irradiance of 20 μmol photons m^{-2} s^{-1}, the maximum C specific CO_2 fixation rate given by equation (11) would be 12.3 10^{-6} s^{-1} = 0.044 h^{-1}. The achieved rate will be slightly lower due to light-dependent reductions of the photon efficiency. Assuming the photosynthesis vs. irradiance relationship given in equation (2), the degree of light-dependent reduction of photon efficiency is given by:

$$\frac{\phi}{\phi m} = \frac{E_K}{E}\left(1 - \exp\left(\frac{-E}{E_K}\right)\right) \qquad (12)$$

For $P_m^C = 4.5\,10^{-5}$ s^{-1}, the CO_2 fixation rate at 20 μmol photons m^{-2} s^{-1} is 10.7 10^{-6} s^{-1} = 0.039 h^{-1}. Thus, even at this low irradiance, which is only sufficient to achieve about 25% of the light-saturated maximum rate, the photon efficiency is about 87% of the maximum. Such

Downloaded By: [Geider, Richard J.] At: 09:45 19 November 2009

calculations of the reduction of ϕ with increasing E (equation (12)) will clearly depend on the precise shape of the photosynthesis vs. irradiance curve, for which several alternative equations could provide different empirical approximations (Falkowski and Raven 2007).

Photoacclimation of light harvesting

The chlorophyll *a* to carbon ratio and the proportion of cellular C accounted for by the light-harvesting components of thylakoid membranes declines in high light (Figure 4). This decline is usually attributed to a requirement to reduce the potential for oxidative stress by reducing the biomass-specific rate of light absorption. This reduction of Chl:C occurs while growth is still light limited. Significantly, in *Dunaliella tertiolecta*, as in other microalgae, the reduction in the light-harvesting components is not accompanied by an increase in the Calvin cycle enzyme RuBisCO (Sukenik et al. 1987; Fisher et al. 1989; Six et al. 2008; Harris et al. 2009), nor in the cell-specific light-saturated photosynthesis rate (Myers and Graham 1971; Sukenik et al. 1987).

Capital costs of CO_2 fixation at light saturation

Turning to the light-saturated rate of CO_2 fixation, we need to consider both the capacity of the thylakoid membranes to generate NADPH and ATP and the capacity of the Calvin cycle to use these products of the light reactions to fix CO_2. As a specific example, consider a spherical phytoplankton cell with a volume of 150 μm^3 (diameter = 3.3 μm) and organic carbon content of 30 pg C. To grow at a specific growth rate of 2.5 d^{-1} at 25 °C in continuous light, such a cell must have a net photosynthesis rate of about 72 amol CO_2 $cell^{-1}$ s^{-1}. If 20% of the gross CO_2 fixation is respired during biosynthesis and maintenance, then a gross CO_2 fixation rate of about 90 amol CO_2 $cell^{-1}$ s^{-1} is required. To support this rate of CO_2 fixation requires generation of 180 amol NADPH $cell^{-1}$ s^{-1} and 360 amol ATP $cell^{-1}$ s^{-1}, which in turn requires a LPET rate of 360 amol e^- $cell^{-1}$ s^{-1} and a minimum CPET rate of 150 amol e^- $cell^{-1}$ s^{-1} (assuming the most efficient mechanisms of NADPH and ATP synthesis). Significantly higher rates of LPET (and lower CPET) may occur at saturating light if the water-water cycle acts as a significant sink for excitation energy (Asada 1999).

The minimum cellular requirements for RCII, RCI and RuBisCO can be calculated from the LPET, CPET and CO_2 fixation rates using information on the maximum catalytic efficiencies of RCII, RCI and RuBisCO. Given a minimum RCII turnover time (for whole chain LPET) of about 2 ms (e.g. maximum e^- transfer rate of 500 e^- $RCII^{-1}$ s^{-1}) and RCI turnover time of about 1 ms for RCI (e.g. maximum e^- transfer rate of 1000 e^- $RCII^{-1}$ s^{-1}), the cellular amounts of RCI and RCII required to achieve a gross photosynthetic rate of 90 amol CO_2 $cell^{-1}$ s^{-1} are 0.72 amol RCII $cell^{-1}$ and 0.51 amol RCI $cell^{-1}$. Using a V_{max} for RuBisCO of 30 mol CO_2 (mol RuBisCO)$^{-1}$ s^{-1} (Evans and Seemann, 1989), the RuBisCO requirement to support a CO_2 fixation rate of 90 amol CO_2 $cell^{-1}$ s^{-1} is 3 amol RuBisCO $cell^{-1}$. The stroma contains the Calvin cycle enzymes and other enzymes including carbonic anhydrase, which facilitates the supply of CO_2 to the Calvin cycle. The carboxylating enzyme RuBisCO makes the largest contribution to the mass of the stroma due to its large size and low catalytic rate. Given a MW of 560,000 for RuBisCO, the cellular requirement is 1.85 pg RuBisCO $cell^{-1}$, accounting for about 3% of cellular C. Taking account of the other Calvin cycle enzymes and carbonic anhydrase, it is likely that about 5% of cellular C would be required for the catalysts of the photosynthetic dark reactions.

The values calculated in the preceding paragraph can be compared with observations for *Dunaliella tertiolecta*, which conveniently has a cell carbon content of about 30 pg C $cell^{-1}$ (see legend to Figure 4). A maximum RCII turnover rate of about 280 e^- $RCII^{-1}$ s^{-1} was reported by Sukenik et al. (1987) for *D. tertiolecta* at a temperature of 18 °C. At this temperature, the cellular contents of RCII and RCI were about 0.7 amol RCII $cell^{-1}$and 0.9 amol RCI $cell^{-1}$ at the highest photon flux density employed in the study (1900 μmol photons m^{-2} s^{-1}). Cellular contents of these reaction centres were higher at lower growth irradiances (see Figure 4). The measured cellular content of RuBisCO in *D. tertiolecta* at 18 °C was 3.3 amol $cell^{-1}$, independent of the growth irradiance, and the achieved catalytic rate during light-saturated photosynthesis was about 12 mol CO_2 (mol RuBisCO)$^{-1}$ s^{-1} (Sukenik et al. 1987). The lower temperature employed in the experimental study (18 °C) may account for much of the difference between the observed catalytic rates and the rates assumed for 25 °C (Raven and Geider 1988). However, other features of the observations deserve comment. In particular, the observed RCI:RCII of 1.3 mol RCI (mol RCII)$^{-1}$ relative to the calculated ratio of 0.71 suggests that RCII is operating at a higher proportion of its maximum rate than RCI or that the ratio of CPET/LPET was higher than assumed.

Cost–benefit considerations in phytoplankton growth

The previous section considered design constraints on the rate and efficiency of CO_2 fixation by chloroplasts. To extend this cost–benefit approach from chloroplasts to phytoplankton cells, the framework of energetic efficiency, catalytic efficiency and safety identified by Raven (1980a) needs to be extended. Over time scales of generations, phytoplankton must achieve the optimal trade-offs amongst (1) increasing acquisition of resources from the environment, (2) retaining these resources within the cells, and (3) utilising these resources efficiently for biosynthesis and growth. A mechanistically informed treatment of trade-offs between costs and benefits would involve four types of costs: capital investments, running costs, opportunity costs and taxes.

The analogy of a chloroplast to a factory is fairly straightforward and useful in examining chloroplast

Downloaded By: [Geider, Richard J.] At: 09:45 19 November 2009

function (Raven 1980a). A raw material (CO_2) is converted into a product (triose-P) using the energy derived from light. The capital investment in this 'factory' consists of the thylakoids and stroma. The running costs are the photons required for NADPH and ATP production. Although it is common to refer to 'cell factories' in the biotechnological context of converting substrates into high value products, the analogy is strained when the product is more cells. Here, it may be difficult to distinguish between capital and product because the product is more capital. Nonetheless, it is useful to consider capital costs as the investment in the long-lived components of a cell and running costs as expenses involved in manufacturing more cells.

Capital costs

Capital is invested in the enzymes, pigments, structural and genetic materials within the cell. The intracellular capital costs are readily quantifiable in terms of the masses of C, N, P, Fe invested in different cellular components. For understanding the roles of phytoplankton in ocean ecosystems and biogeochemistry, the number of components needs to be large enough to describe several competing functions, but small enough to be tractable. To this end, we can suggest the following structural and functional components (see Figure 5): cell wall, cell membrane, light-harvesting and photosynthetic apparatus, photoprotective apparatus, and biosynthetic apparatus. A cell wall and other structural components are required to provide structural integrity and protection from mechanical stress. The plasma membrane provides the interface between the cell and the environment, and provides the surface in which the transporters required for nutrient uptake are embedded. The light-harvesting and photosynthetic apparatus converts light energy into chemical energy and provides the carbon skeletons required for biosynthesis. The photo-protective apparatus provides protection from photo-oxidative stress. Finally, the biosynthetic apparatus produces new cells from inorganic nutrients using energy and carbon skeletons provided by the photosynthetic apparatus. In addition to the compartments illustrated in Figure 5, cells contain genetic material and metabolites.

The sizes of different functional components of a phytoplankton cell can be quantified in terms of the change in the proportions of cellular carbon, (and other elements) that are allocated to the different components. The amount of capital that must be invested in different components to achieve a specified growth rate depends on the maximum catalytic efficiency of the component, and the degree to which this maximum catalytic efficiency is achieved under different environmental conditions. Investment in capital requires biosynthesis, which in the light can use the photosynthate (e.g. triose-P) generated by the Calvin cycle. Biosynthesis in darkness requires that carbon first be stored as starch (or lipid) during the light for subsequent mobilisation in darkness. Thus, in addition to the functional pools, we need to account for a pool of carbon storage polymers (Figure 5). Capital costs can also be calculated in terms of

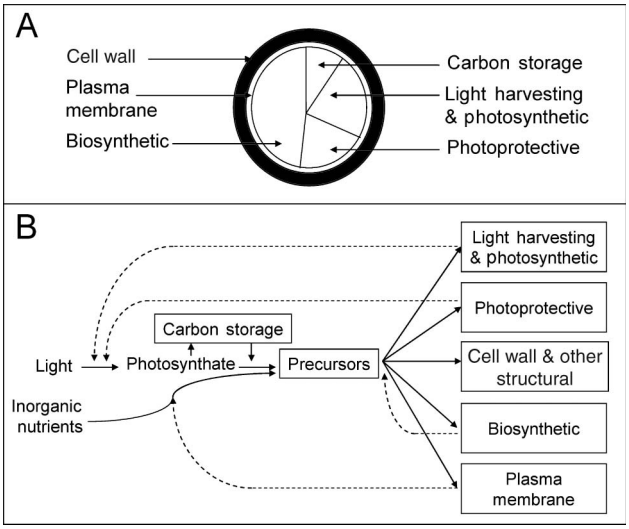

Figure 5. (A) Pie chart of the components of a model phytoplankton cell. (B) Flow of materials (solid arrows) through the components of a model phytoplankton cell, illustrating the processes that different components influence (dashed arrows). The cell wall provides rigidity, but also some protection from grazers. The photosynthetic apparatus includes the thylakoid membranes and Calvin cycle enzymes. The photoprotective component may include the enzymes involved in the D1 repair cycle, the pigments and enzymes involved in non-photochemical excitation energy quenching, and the enzymes involved in removing reactive oxygen species. The biosynthetic apparatus includes the enzymes and ribosomes involved in biosynthesis and protein synthesis. Finally, the plasma membrane houses the nutrient transporters. For a complete model of the phytoplankton cell, to these components should be added low molecular weight intermediates, compatible solutes and nutrient stores (e.g. nitrate in vacuoles, polyphosphate, ferritin).

biovolume of cell as a whole and cell components, the surface areas of membranes, or the amounts of energy contained in the organic matter (which can ultimately be traced to the number of photons required to provide the carbon substrates and energy for photosynthesis, nutrient acquisition and biosynthesis). Geometrical considerations may constrain the absolute and relative sizes of different components. For example, both the cell wall and the plasma membrane will scale with the surface area of the cells. The minimum cell size for a photoautotroph is set by such constraints due to non-scalable components, which contribute an increasing proportion of cell volume as size declines (Raven 1999). Membranes, which have finite thickness of about 5–10 nm, and the minimum genome size are such non-scalable components (Raven 1999). Although small cell size increases the surface area-to-volume ratio and thus the potential for nutrient acquisition, it comes at the expense of an increase in the proportion of non-scalable components.

Running costs

The running costs for CO_2 assimilation were considered in the section on 'Cost benefit analysis of chloroplast function'. In addition to these costs, are the running costs

Downloaded By: [Geider, Richard J.] At: 09:45 19 November 2009

associated with nutrient assimilation and biosynthesis. Nutrient acquisition requires active transport from low concentrations in the environment to high intracellular concentrations, which consumes energy (Raven 1980b; Button 1998). In addition, some unicells produce extracellular products, for example carbonic anhydrase or siderophores to increase resource acquisition. These products have a limited useful life if they diffuse away from the cell, and hence may be counted as running costs. The theoretical basis for assessing the cost of biosynthesis was formalised by Penning de Vries et al (1974) as discussed more recently by Amthor (2000). Biosynthesis costs include the net ATP and reductant demands, which can be calculated from knowledge of biosynthetic pathways, and the costs associated with 'tool use': these include the costs involved in turnover of mRNA and rRNA (Penning de Vries et al. 1974). The cost of synthesis and degradation of transit peptides is another biosynthetic cost. For example, many of the pigment-protein complexes are encoded in the nucleus, synthesised in the cytoplasm and transported to the chloroplast, which requires a transit peptide that is cleaved and degraded to its component amino acids.

Another category of running costs arises from light-induced photo-oxidative stress. Reactive oxygen species (ROS) generated by light include singlet oxygen, peroxide, superoxide radicals and hydroxide radicals. Photoautotrophs employ mechanisms for the controlled production of ROS, for example by the Mehler reaction, and the controlled disposal of ROS using antioxidants and associated enzyme systems (Asada 1999; Logan et al. 2006). In addition to production and disposal of ROS via the water–water cycle, ROS are produced as a consequence of the interaction of light with pigments (Falkowski and Raven 2007). For example, singlet O_2 is produced via resonance energy transfer from triplet excited state chlorophyll. The rates of photo-oxidative damage and the costs associated with repairing damaged proteins, pigments and lipids have been poorly quantified. One process that has been quantified is photoinhibition of RCII function (Raven and Samuelsson 1986; Raven 1989): however, this cost appears to be relatively small compared with the energy required to support light-saturated photosynthesis (Raven and Samuelsson 1986).

The rate of production of ROS can be reduced by decreasing cellular chlorophyll *a* content and Chl:C, thus reducing the rate of light absorption. Up-regulation of non-photochemical excitation energy quenching can also be used to reduce the rate of photoinhibition and generation of ROS. The requirement for repair can also be reduced by investment of capital in up-regulation of ROS scavenging systems. It is likely that the trade-offs amongst reducing light harvesting, up-regulating non-photochemical quenching mechanisms and up-regulating ROS scavenging systems will depend not only on the mean irradiance but also on the variability of the light environment including the maximum irradiance encountered and the frequency of fluctuations (Moore et al. 2006). Additionally, the availability of other limiting resources, including nutrients, may again play a role in moderating susceptibility to photoinhibition. However, interactions are likely to be complex and remain to be fully elucidated (Kolber et al. 1994; Moore et al. 2007; Bailey et al. 2008; Mackey et al. 2008).

Opportunity costs

Opportunity costs are associated with the diversion of resources from one functional pool in order to increase the capacity of another. An opportunity cost is the value of foregone opportunities unrealised because of the resources devoted towards an alternative option. For example, diversion of resources from Calvin cycle enzymes and/or ribosomes to the light-harvesting apparatus in low-light environments (i.e. scenarios 1 and 2 considered above) may reduce the opportunity to exploit intermittent exposure to high light in an otherwise light-limited environment such as a deeply mixed layer. Thus, the extent to which pigment content increases during prolonged growth in a low-light environment such as the deep chlorophyll maximum layer may be subject to a constraint that the cells retain the capacity to rapidly respond to increases in light availability. Despite this, obligate low-light and high-light adapted strains of globally signifcant phytoplankton groups have been identified: i.e. deep versus shallow ecotypes of *Prochlorococcus* (Moore and Chisholm 1999) and *Ostreococcus* (Rodríguez et al. 2005).

In the light environment experienced in nature, cells may be exposed to both light-saturating and light-limiting conditions due to changes of position within a vertical light gradient. In a chronically light-limited environment, such as a deep wind-mixed layer, cells may nonetheless be intermittently exposed to saturating light (MacIntyre et al. 2000). The variable, often punctuated, nature of the natural light environment complicates a cost–benefit analysis of pigment acclimation because capital, running and opportunity costs may be interdependent. For example, diversion of resources from Calvin cycle enzymes to light-harvesting pigment–protein complexes will decrease the opportunity cost of intermittent exposure to high light whilst simultaneously increasing the running cost associated with repair of damage caused by intermittent exposure to high light. Overall it could thus be hypothesised that the apparent insensitivity of light-saturated photosynthesis to growth irradiance (e.g. Myers and Graham 1971; Sukenik et al 1987; Fisher et al. 1989; Harris et al. 2009) may be an evolutionary consequence of light variability within the mixed layer.

Taxes

Finally, we can also differentiate between taxes, which are imposed on the cell from outside, and the running costs involved in maintenance and repair of damage generated within the cell. Thus, by taxes we are primarily concerned with losses due to grazing, disease and sinking. To date, cost–benefit considerations have been applied in modelling

Downloaded By: [Geider, Richard J.] At: 09:45 19 November 2009

resource acquisition by phytoplankton (Shuter 1979; Pahlow 2005) and are therefore most applicable to reproduction (r-) strategies, which involve investment in the photosynthetic and biosynthetic components to maximise cell division rate. Less attention has been paid to persistence (K-) strategies, which involve investment in walls and other defence mechanisms to reduce losses to grazers (Raven and Waite 2004). Robust cell walls (Hamm et al. 2002), production of alleochemicals and extracellular polymers (Wolfe et al. 1997; Wolfe 2000) may all deter grazers and will all presumably require some investment of both material and energy. The benefits of an r-strategy are quantified in terms of the increase in resource acquisition rates, which can be readily measured. Quantifying the reduction in grazing pressure due to an investment in anti-predation mechanisms may be more difficult.

Conclusion

Developing a predictive understanding of the roles of phytoplankton in biogeochemical cycles depends on understanding how some genotypes come to make disproportionate contributions to ocean biogeochemistry. Thus, one of the foci in phytoplankton growth models needs to be elucidation of traits that lead to periods of dominance within a seasonal cycle (e.g. blooms), or in different ocean biogeochemical provinces (Follows et al. 2007). Models that account for the optimal allocation of resources to competing functions provide one approach for gaining a predictive understanding of how phytoplankton exploit the resources and cope with the stresses inherent in their environment.

In applying optimality models to phytoplankton ecology, defining the fitness function that is to be maximised is crucial. To date, optimality models of phytoplankton growth have defined fitness in the relatively narrow sense of maximising the cell division rate by maximising resource acquisition through adjustment of Chl:C, N:C and N:P (Shuter 1979; Klausmeir et al. 2004; Pahlow 2005; Armstrong 2006; Pahlow and Oschlies 2009). These models can improve our understanding of phenotypic/physiological responses, which occur on time scales of hours to days. Although the benefits of adjusting elemental composition and pigment content have been well articulated and are explicit, often the costs have not been treated in a similar explicit manner.

The evolutionary history should also be appreciated when considering phenotypic responses. For example, at least some components of the photosynthetic apparatus appear to be sub-optimal 'frozen metabolic accidents' consisting of fundamental molecular building blocks which are ancient and highly conserved (Shi et al. 2005; Shi and Falkowski 2008). The complex and potentially variable phenotypic acclimation responses which have evolved in response to environmental variability could thus be considered as mechanisms to cope with the sub-optimal nature of these components of the molecular machinery (Falkowski et al. 2008). Consequently caution should perhaps be applied when using optimality based arguments to describe phenotypic responses.

On the other hand, the task of model building may actually be easier if the scope for adaptation is constrained by a high degree of conservation in the catalysts involved in LPET and CO_2 fixation. Raven (1980a, p. 199) noted the basic similarities within eukaryotic chloroplasts and concluded that "the great range and ecological categories of eukaryotic micro-algae is achieved largely by altering the quantity of the various components of the chloroplasts, and the ratio of chloroplast material to the rest of the cell". This may facilitate use of optimality considerations within the constraints imposed by the 'metabolic accidents' of evolutionary history. Photoacclimation of pigment content appears to be universal within the microalgae, and mechanistic explorations of the costs and benefits of this acclimation should lead to improved understanding of phytoplankton ecophysiology.

Minimisation of loss terms, for example by avoiding grazers, may often be as important as growth optimisation in structuring phytoplankton communities (Smetacek et al. 2004). Although the benefits of avoiding being eaten are self-evident, the costs associated with predator avoidance have been given little attention in phytoplankton growth models. In this context, the traits that allow some genotypes to persist without forming blooms may be as interesting as the traits that allow other genotypes to bloom.

In conclusion, although optimality arguments are likely to be a powerful tool that will be employed in the next generation of phytoplankton-biogeochemical models, the development of fitness functions for these models will require a sound mechanistic basis. In particular, the interactions amongst multiple factors relevant to the time and space scales of interest will have to be considered. Finally, individual fitness functions should ideally be amenable to experimental verification or falsification of the assumed underlying physiological and ecological process.

Acknowledgements

The authors acknowledge financial support from the NERC funded MarQUEST initiative as part of the larger QUEST consortium. ONR was supported through a Spanish CSIC JAE postdoctoral fellowship. CMM was supported by a NERC postdoctoral Fellowship. We also acknowledge a thought-provoking review by Michael Behrenfeld and the comments of two anonymous referees.

Notes on contributors

Richard J. Geider is a Professor of Biology at the University of Essex. His research interests are in marine primary productivity and phytoplankton ecophysiology, particularly in how phytoplankton adapts to physical/chemical resource limitations. His research combines the insights gained from laboratory studies employing unialgal cultures and field work on natural phytoplankton assemblages to understand the role of phytoplankton in ocean biogeochemistry.

C. Mark Moore is an academic fellow at the National Oceanography Centre, University of Southampton with research interests in

Downloaded By: [Geider, Richard J.] At: 09:45 19 November 2009

phytoplankton ecophysiology and ocean biogeochemistry. His research principally involves the use of interdisciplinary field data sets, sometimes augmented with laboratory studies or simple theoretical models, to investigate the physical causes and biogeochemical consequences of resource limitation of marine phytoplankton.

Oliver N. Ross is currently a postdoctoral researcher at the CMIMA in Barcelona, Spain. His primary research interests include cross-disciplinary processes in the ocean (turbulent mixing and the vertical fluxes of nutrients and algal carbon, the influence of turbulence on phytoplankton photoacclimation and primary production and the formation of thin layers). He currently works on refining hyperspectral optical methods for the detection and characterisation of phytoplankton species and dynamical processes.

References

Aksens DL, Egge JK. 1991. A theoretical model for nutrient transport in phytoplankton. Marine Ecology Progress Series 70:65–72.

Amthor JS. 2000. The McCree – de Wit-Penning de Vries-Thornley respiration paradigms: 30 years later. Annals of Botany 86:1–20.

Armstrong RA. 2006. Optimality-based modelling of nitrogen allocation and photoacclimation in photosynthesis. Deep-Sea Research II 53:513–531.

Asada K. 1999. The water–water cycle in chloroplasts: scavenging of active oxygen and dissipation of excess photons. Annual Reviews of Plant Physiology and Plant Molecular Biology 50:601–639.

Aumont O, Maier-Reimer E, Blain S, Monfray P. 2003. An ecosystem model of the global ocean including Fe, Si, P colimitations. Global Biogeochemical Cycles 17(2): doi:10.1029/2001GB001745.

Bailey S, Melis A, Mackey KRM, Cardol P, Finazzi G, van Dijken G, Berg GM, Arrigo K, Shrager J, Grossman A. 2008. Alternative photosynthetic electron flow to oxygen. Biochimica et Biophysica Acta 1777:269–276.

Baker NR, Harbinson J, Kramer DM. 2007. Determining the limitations and regulation of photosynthetic energy transduction in leaves. Plant, Cell and Environment 30:1107–1125.

Behrenfeld MJ, Halsey KH, Milligan AJ. 2008. Evolved physiological responses of phytoplankton to their integrated growth environment. Philosophical Transactions of the Royal Society B 363:2687–2703.

Behrenfeld MJ, Prasil O, Babin M, Bruyant F. 2004. In search of a physiological basis for covariations in light-limited and light-saturated photosynthesis. Journal of Phycology 40:4–25.

Berner T, Dubinsky Z, Wyman K, Falkowski PG. 1989. Photoadaptation and the package effect in *Dunaliella tertiolecta* (Chlorophyceae). Journal of Phycology 25:70–78.

Blackenship RE. 2002. Molecular mechanisms of photosynthesis. Oxford: Blackwell.

Button DK. 1998. Nutrient uptake by microorganisms according to kinetic parameters from theory as related to cytoarchitecture. Microbial Molecular Biology Reviews 62:636–645.

Doney SC, Keith LK, Moore JK. 2003. Global ocean carbon cycle modeling. In: Fasham MFR, editor. Ocean biogeochemistry: The role of the ocean carbon cycle in global change. Berlin, Heidelberg, New York: Springer-Verlag. p. 217–238.

Evans JR, Seemann JR. 1989. The allocation of protein nitrogen in the photosynthetic apparatus: costs, consequences and control. Photosynthesis. New York: Alan R. Liss Inc. p. 183–205.

Falkowski PG, Barber RT, Smetacek V. 1998. Biogeochemical controls and feedbacks on ocean primary production. Science 281:200–206.

Falkowski PG, Fenchel T, Delong EF. 2008. The microbial machines that drive Earth's biogeochemical cycles. Science 320:1034–1038.

Falkowski PG, Owens TG. 1980. Light-shade adaptation – two strategies in marine phytoplankton. Plant Physiology 66:592–595.

Falkowski PG, Raven JA. 2007. Aquatic photosynthesis. 2nd Edition. Princeton: Princeton University Press.

Fisher T, Shurtz-Swirski R, Gepstein S, Dubinsky Z. 1989. Changes in the levels of ribulose-1,5-bisphosphate carboxylase/oxygenase (RUBISCO) in *Tetraedron minimum* (Chlorophyta) during light and shade adaptation. Plant Cell Physiology 30:221–228.

Flynn KJ. 2001. A mechanistic model for describing dynamic multi-nutrient, light, temperature interactions in phytoplankton. Journal of Plankton Research 23:977–997.

Flynn KJ. 2003. Do we need complex mechanistic photoacclimation models for phytoplankton? Limnology and Oceanography 48:2243–2249.

Follows MJ, Dutkiewicz S, Scott GS, Chisholm SW. 2007 Emergent biogeography of microbial communities in a model ocean. Science 315:1843–1846.

Friend AD, Geider RJ. Behrenfeld MJ, Still CJ. 2009. Photosynthesis in global-scale models. In: Laisk A, Nedbal L, Govindjee, editors. Towards photosynthesis in silico. Dordrecht: Springer. p. 465–497

Hamm CE, Merkel R, Springer O, Jurkojc P, Maier C, Pretchel K, Smetacek V. 2002. Architecture and material properties of diatom shells provide effective mechanical protection. Nature 421:841–843.

Harris GN, Scanlan DJ, Geider RJ. 2009. Responses of *Emiliania huxleyi* (Prymnesiophyceae) to step changes in photon flux density. European Journal of Phycology 44:31–48.

Harris GP. 1986. Phytoplankton ecology: structure, function and fluctuations. London: Chapman & Hall.

Hood RR, Laws EA, Follows MJ, Siegel DA. 2007. Modeling and prediction of marine microbial populations in the genomic era. Oceanography 20:155–167.

Klausmeier CA, Litchman E, Daufresne T, Levin SA. 2004. Optimal nitrogen-to-phosphorus stoichiometry of phytoplankton. Nature 429:171–174.

Kolber ZS, Barber RT, Coale KH, Fitzwater SE, Greene RM, Johnson KS, Lindley S, Falkowski PG. 1994. Iron limitation of phytoplankton photosynthesis in the equatorial Pacific-Ocean. Nature 37:145–149.

Kramer DM, Avenson TJ, Edwards GE. 2004. Dynamic flexibility in the light reactions of photosynthesis governed by both electron and proton transfer reactions. Trends in Plant Science 9:349–357.

Litchman E, Klausmeier CA, Schofield OM, Falkowski PG. 2007. The role of functional traits and trade-offs in structuring phytoplankton communities: scaling from cellular to ecosystem level. Ecology Letters 10:1170–1181.

Logan BA, Kornyeyev D, Hardison J, Holaday AS. 2006. The role of antioxidant enzymes in photoprotection. Photosynthesis Research 88:119–132.

MacIntyre HL, Kana TM, Geider RJ. 2000. The effect of water motion on short-term photosynthesis by marine phytoplankton. Trends in Plant Science 5:12–17.

Mackey KRM, Paytan A, Grossman AR, Bailey S. 2008. A photosynthetic strategy for coping in a high-light, low-nutrient environment. Limnology and Oceanography 53:900–913.

Moore CM, Seeyave S, Hickman AE, Allen JT, Lucas MI, Planquette H, Pollard RT, Poulton AJ. 2007. Iron-light interactions during the CROZet natural iron bloom and EXport experiment (CROZEX) I: Phytoplankton growth and photophysiology. Deep-Sea Research II 54:2045–2065.

Downloaded By: [Geider, Richard J.] At: 09:45 19 November 2009

Moore CM, Suggett DJ, Hickman AE, Kim YN, Tweddle JF, Sharples J, Geider RJ, Holligan PM. 2006. Phytoplankton photoacclimation and photoadaptation in response to environmental gradients in a shelf sea. Limnology and Oceanography 51:936–949.

Moore JK, Doney SC, Lindsay K. 2004. Upper ocean ecosystem dynamics and iron cycling in a global three-dimensional model. Global Biogeochemical Cycles 18: GB4028.

Moore LR, Chisholm SW. 1999. Photophysiology of the marine cyanobacterium *Prochlorococcus*: ecotypic differences among cultured strains. Limnology and Oceanography 44:628–638.

Myers J. 1980. On the algae: thoughts about physiology and measurements of efficiency. In: Falkowski PG, editor. Primary productivity in the sea. New York: Plenum Press. p. 1–15.

Myers J, Graham J-R. 1971. The photosynthetic unit in Chlorella measured by repetitive short flashes. Plant Physiology 48:282–286.

Pahlow M. 2005. Linking chlorophyll-nutrient dynamics to the Redfield N:C ratio with a model of optimal phytoplankton growth. Marine Ecology Progress Series 287:33–43.

Pahlow M, Oschlies A. 2009. Chain model of phytoplankton P, N and light colimitation. Marine Ecology Progress Series 376:69–83.

Penning de Vries FWT, Brunsting AHM, van Laar HH. 1974. Products, requirements and efficiency of biosynthesis: a quantitative approach. Journal of Theoretical Biology 45:339–377.

Raven JA. 1980a. Chloroplasts of eukaryotic micro-organisms. In: Gooday GW, Lloyd D, Trinci APJ, editors. The eukaryotic microbial cell – 13th Symposium of the Society for General Microbiology. Cambridge: Cambridge University Press. p. 181–205.

Raven JA. 1980b. Nutrient transport in microalgae. Advances in Microbial Physiology 21:47–226.

Raven JA. 1984. A cost–benefit analysis of photon absorption by photosynthetic unicells. New Phytologist 98:593–625.

Raven JA. 1988. The iron and molybdenum use efficiencies of plant growth with different energy, carbon and nitrogen sources. New Phytologist 109:279–287.

Raven JA. 1989. Fight or flight: the economics of repair and avoidance of photoinhibition of photosynthesis. Functional Ecology 3:5–19.

Raven JA. 1990. Predictions of Mn and Fe use efficiencies of phototrophic growth as a function of light availability for growth and of C assimilation pathway. New Phytologist 116:1–18.

Raven JA. 1997. Inorganic carbon acquisition by marine autotrophs. Advances in Botanical Research 27:85–209.

Raven JA. 1999. Picophytoplankton. Progress in Phycological Research 13:33–106.

Raven JA, Cockell CS, De La Rocha CL. 2008. The evolution of inorganic carbon concentrating mechanisms in photosynthesis. Philosophical Transactions of the Royal Society London B 363:2641–2650.

Raven JA, Caldera K, Elderfield H, Hoegh-Guldberg O, Liss, P, Riebesell U, Shepherd J, Turley C, Watson A. 2005. Ocean acidification due to increasing atmospheric carbon dioxide. London: The Royal Society. Policy Document 12/05.

Raven JA, Geider RJ. 1988. Temperature and algal growth. New Phytologist 110: 441–461.

Raven JA, Handley LL. 1987. Transport processes and water relations. New Phytologist 106(supplement):217–233.

Raven JA, Johnston AM. 1991. Mechanisms of inorganic carbon acquisition in marine phytoplankton and their implications for the use of other resources. Limnology and Oceanography 36:1701–1717.

Raven JA, Richardson K. 1984. Dinoflagellate flagella: a cost–benefit analysis. New Phytologist 98:259–276.

Raven JA, Samuelsson G. 1986. Repair of photoinhibitory damage in *Anacystic nidulans* 625 (*Synechococcus* 6301): relation to catalytic capacity for, and energy supply to, protein synthesis, and implications for μ_{max} and the efficiency of light-limited growth. New Phytologist 103:625–643.

Raven JA, Waite AM. 2004. The evolution of silicification in diatoms: inescapable sinking and sinking as escape? New Phytologist 162:45–61.

Rodríguez F, Derelle E, Guillou L, Le Gall F, Vaulot D, Moreau H. 2005. Ecotype diversity in the marine picoeukaryote *Ostreococcus* (Chlorophyta, Prasinophyta). Environmental Microbiology 7:853–859.

Ross ON, Geider RJ. 2009. A cell-based model of photosynthesis and photo-acclimation based on the accumulation and mobilisation of energy reserves in phytoplankton. Marine Ecology Progress Series 383:53–71.

Shi T, Bibby T, Jiang L, Irwin A, Falkowski PG. 2005. Protein interactions limit the rate of evolution of photosynthetic genes in cyanobacteria. Molecular Biology and Evolution 22:2179–2189.

Shi T, Falkowski PG. 2008 Genome evolution in cyanobacteria: the stable core and the variable shell. Proceedings of the National Academy of Sciences USA 105:2510–2515.

Shuter B. 1979. Model of physiological adaptation in unicellular algae. Journal of Theoretical Biology 78:519–552.

Six C, Finkel ZV, Rodriguez F, Dominique D. Pertensky F, Campbell DA. 2008. Contrasting photoacclimation costs in ecotypes of the marine eukaryotic picoplankter *Ostreococcus*. Limnology and Oceanography 53:255–265.

Smetacek V, Assmy P, Henjes J. 2004. The role of grazing in structuring Southern Ocean pelagic ecosystems and biogeochemical cycles. Antarctic Science 16:541–558.

Sukenik A, Bennett J, Falkowski P. 1987. Light-saturated photosynthesis – limitation by electron transport or carbon fixation? Biochemica et Biophysica Acta 891:205–215.

Westberry T, Behrenfeld MJ, Siegel DA, Boss E. 2008. Carbon-based primary productivity modeling with vertically resolved photoacclimation. Global Biogeochemical Cycles 22:GB2024, doi:10.1029/2007GB003078.

Wolfe GV. 2000. The chemical defense ecology of marine unicellular plankton: constraints, mechanisms, and impacts. Biological Bulletin 198:225–244.

Wolfe GV, Steinke M, Kirst GO. 1997. Grazing-activated chemical defence in a unicellular marine alga. Nature 387:894–897.

Downloaded By: [Geider, Richard J.] At: 09:45 19 November 2009